

# Nominal doping and partition of doped holes between planar and apical orbitals in $\text{La}_{2-x}\text{Sr}_x\text{CuO}_4$

E. S. Božin<sup>1</sup> and S. J. L. Billinge<sup>1,2</sup>

<sup>1</sup> *Department of Physics and Astronomy and Center for Fundamental Materials Research, Michigan State University, East Lansing, MI 48824-1116.*

<sup>2</sup> *Istituto Nazionale di Fisica della Materia, Dipartimento di Fisica,*

*Università di Roma, "La Sapienza" Piazzale Aldo Moro, 2, I-00185 Roma, Italy. \**

(Dated: May 22, 2019)

Using structural data from neutron powder diffraction, we have tested the novel hypothesis by Perry *et al.* [Perry *et al.*, Phys. Rev. B **65**, 144501 (2002)] that doping in the  $\text{La}_{2-x}\text{Sr}_x\text{CuO}_4$  system occurs as localized defects, of predominantly  $\text{Cu}d_{3z^2-r^2}\text{-Op}_z$  character, associated with dopant Sr ions. The structural parameters behave qualitatively according to the prediction of this model. A more quantitative analysis indicates that doped holes predominantly appear in the planar  $\text{Cu}d_{x^2-y^2}\text{-Op}_{x,y}$  band as is normally assumed. A small amount of the doped charge does enter the  $\text{Cu}d_{3z^2-r^2}\text{-Op}_z$  orbitals. This has been estimated for all values of  $x$  using bond-valence methods.

PACS numbers: 74.81.-g, 74.72.Dn, 74.72.-h, 61.12.-q

Cuprate high temperature superconductors are doped Mott insulators. The novel superconductivity appears at doping levels just beyond the insulator-metal (IM) transition. The insulating behavior of the undoped endmember is understood to be due to electron correlation effects in the half-filled planar  $\text{Cu}d_{x^2-y^2}\text{-Op}_\alpha$  ( $\alpha = x, y$ ) anti-bonding band. The phase diagram of the cuprates can be interpreted in terms of holes doped into this planar band. For example, in the system  $\text{La}_{2-x}\text{Sr}_x\text{CuO}_4$  it is assumed that one hole enters this band per strontium atom. This paradigm for the doping has hardly been questioned and a multitude of papers exist implicitly assuming this behavior. The  $\text{La}_{2-x}\text{Sr}_x\text{CuO}_4$  system is archetypal since it is a single layer system which can be straightforwardly doped over a wide range. The resulting phase diagram is thought to exhibit features that are universal to the cuprates. However, as a result of recent *ab initio* electronic band structure calculations, Perry, Tahir-Kheli and Goddard (PTG) [1] have suggested a new model for the doping in the  $\text{La}_{2-x}\text{Sr}_x\text{CuO}_4$  system. In this case the doped holes reside in localized states on the  $\text{CuO}_6$  octahedra situated next to the dopant strontium ions. Furthermore, the doped charge resides principally in the  $\text{Cu}d_{3z^2-r^2}\text{-Op}_z$  orbitals (i.e., the out-of-plane bonds). Coincidentally a structural distortion occurs such that the local Jahn-Teller (JT) distortion, that results in the long Cu-O apical bond, is destroyed. A flat impurity band forms in the gap. The IM transition then occurs on increased doping in a manner similar to doped semiconductors by percolation of the doped impurities. These calculations were originally motivated by XAFS measurements that observed a distorted environment of the octahedra in the vicinity of dopant ions [2]. This new way of understanding the doping, if it is right, clearly will result in a paradigm shift in our understanding of cuprate physics. It is thus of the greatest importance to test the hypothesis experimentally. A rather direct

probe of this doping mechanism is the structure because it involves the local destruction of JT elongated bonds. The *average* Cu-O bond length along  $z$  will thus shorten with doping and the width of the bond-length distribution for this bond will increase reflecting the increased disorder. Despite detailed structural studies of this system [3] the temperature and doping dependence of these parameters has not been reported. In this paper we investigate whether there is evidence supporting this new doping paradigm in both the average crystal structure, and the local structure as measured using the atomic pair distribution function (PDF) technique [7]. We reexamine the extensive earlier structural data of Radaelli to extract the desired parameters. We have also analyzed new neutron powder diffraction data using Rietveld refinement and PDF refinement. We find that the data qualitatively agree with the predictions of the Perry *et al.* [1]. However, a more quantitative analysis, including evaluating the bond valences as a function of doping of the in-plane and apical Cu-O bonds, indicates that doped charge is predominantly residing in the planar bonds suggesting the existing paradigm for doping is valid.

This study reexamines the extensive published data of Radaelli *et al.* [3] to extract as a function of doping the interesting parameters of the plane copper to apical oxygen bond length,  $r_{\text{Cu-O}2}$  and the short lanthanum/strontium to apical oxygen bond length,  $r_{\text{La/Sr-O}2}$ . These parameters were determined from the reported fractional coordinates and lattice parameters. Also important is the doping dependence of the copper to in-plane oxygen bond length,  $r_{\text{Cu-O}1}$ , which was presented previously [3] but is reexamined here. To check the PTG prediction we also need the anisotropic displacement parameter along the  $z$ -axis of the apical oxygen,  $U_{33}(\text{O}2)$ . This was not published in [3] so we have used recently collected neutron powder diffraction data of our own from a less extensive set of samples. Samples were synthesized using solid state

methods and loose powders of  $\sim 10$  g sealed in vanadium cylinders were measured at 10 K at the GEM diffractometer at the ISIS neutron source. Details of sample synthesis, characterization and measurement are reported elsewhere [4, 5]. Rietveld refinements were carried out on the data using the program GSAS [6]. The data were also corrected for experimental effects and normalized to obtain the atomic pair distribution function [7] (PDF) using the program PDFgetN [8]. The PDF is the Fourier transform of the normalized corrected powder diffraction data. It utilizes both Bragg and diffuse scattering and contains information about the local structure [7]. Structural models were refined to the PDFs using the program PDFFIT [9]. To check for consistency, the same parameters were varied in the PDF and Rietveld refinements. The PDF allows us to explore models that contain non-periodic defects such as those proposed by PTG. The PDF was calculated of a supercell model including doping induced defects discussed by PTG. This was then used as simulated data and fit using the usual long-range orthorhombic (LTO) [3] structural model. In this way it was possible to estimate the size of enlarged displacement factors that would result from the presence of the doping induced disorder described by PTG. In Perry *et al.* [1] for simplicity no octahedral tilts were considered. In the present case we must compare resulting models with real data and so the doping induced defects described in [1] were superimposed on the background of octahedral tilts observed in the undoped endmember.

The qualitative predictions for the evolution of the average structure with doping in the scenario of Perry *et al.* [1] are: (1) decrease in the average  $r_{Cu-O_2}$  due to the local destruction of Jahn-Teller distortions at  $Cu^{3+}$  sites; (2) increase in the  $U_{33}(O_2)$  with doping because of the coexistence of Jahn-Teller distorted and non-Jahn-Teller distorted octahedra; (3) increase in the average  $r_{La/Sr-O(2)}$  distance. All these effects are seen qualitatively in the data as shown in Figs. 1 and 2. However, similar effects can be expected even if the doping is taking place in the conventional way: homogeneously into the planar bonds. For example, if the  $CuO_2$  planes are becoming more positively charged with doping the negatively charged apical oxygen would be predicted to come closer to the planes due to simple coulomb attraction. Also, the  $U_{33}$  displacement factor of the apical oxygen atom is expected to increase with doping due to the random doping of larger  $Sr^{2+}$  ions. It is therefore important to be more quantitative to distinguish these different possibilities.

The PTG calculations [1] were carried out at special rational doping fractions of 1/8, 1/4 and 1/2 and suggest the appearance of a single distorted  $CuO_6$  octahedron associated with each doped strontium. The  $r_{Cu-O_2}$  bond closest to the strontium is shortened by  $\Delta r_{Cu-O_2} = -0.24$  Å and that farthest from the Sr on the same octahedron by  $\Delta r_{Cu-O_2} = -0.10$  Å, the Sr-O2 dis-

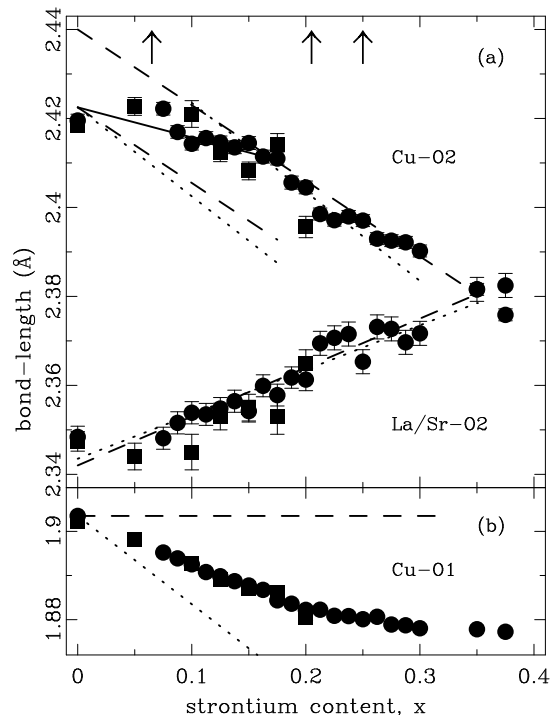


FIG. 1: Evolution of  $r_{Cu-O_2}$  and  $r_{La/Sr-O_2}$  (a), and  $r_{Cu-O_1}$  (b) average bond lengths with hole doping at 10 K: Rietveld result from [3] (solid circles) and PDF result (solid squares). Dotted lines: slope predicted from simple electrostatics considerations. Dashed lines: slope prediction based on PTG model. Arrows (from left to right): IM transition, structural phase transition, and disappearance of superconductivity.

tance increases,  $\Delta r_{La/Sr-O_2} = +0.11$  Å and the in-plane  $r_{Cu-O_1}$  distances do not change. In the average structure these defects are not seen explicitly; however, the distortions will be apparent as a properly weighted change in the average bond-length and an increase in the respective displacement parameters. If we assume that these defects appear as each strontium is doped and are not a special feature of the rational doping fractions studied, we get the following relations for the strontium doping,  $x$ , dependence of the average bond lengths:

$$\Delta r_{Cu-O_2}(x) = -0.17x, \quad \Delta r_{La/Sr-O_2}(x) = 0.11x, \quad (1)$$

where  $x$  is the doping level. These are shown as the dashed lines in Fig. 1. The evolution of  $r_{La/Sr-O_2}$  is in quantitative agreement. The case of  $r_{Cu-O_2}$  is more complicated.  $r_{Cu-O_2}$  decreases much more slowly than the prediction initially on doping. However, beyond a doping level of  $\sim 0.17$  the slope of  $r_{Cu-O_2}$  vs  $x$  increases. In this higher doping region the slope of the PTG line agrees rather well with the data. There is no specific prediction from the PTG calculations for the  $x$ -dependence of  $r_{Cu-O_1}$ , although it is expected to be small since the length of  $r_{Cu-O_1}$  in the defect octahedra does not change and no doping dependent change in lattice parameters

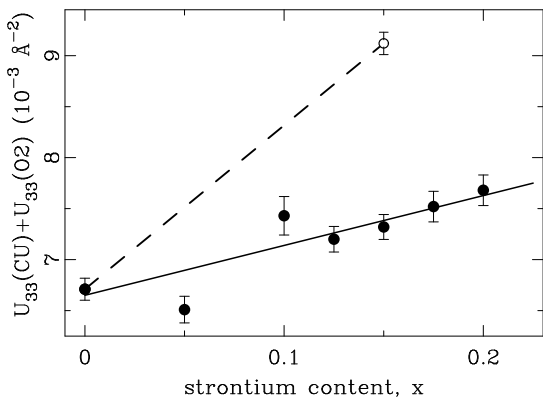


FIG. 2: Sum of displacement parameters  $U_{33}$  for  $Cu$  and  $O2$  as a function of strontium content at 10 K, from PDF refinements. Solid line is a guide to the eye. Dashed line denotes expected increase in the PDF displacement parameters, estimated from PDF simulation based on PTG model for 1/8 doping (see text).

has been assumed in their calculations. This reflects the fact that, in the PTG picture the doped charge is almost exclusively located in the apical  $d_{z^2-r^2}$  orbitals of the copper. Therefore, we have drawn a flat dashed line as the PTG prediction for this parameter in Fig. 1(b). As is apparent, the data for  $r_{Cu-O1}$  slope downward with a slope of  $\Delta r_{Cu-O1} \sim -0.105$ . This is comparable to, though slightly less than, the observed  $\Delta r_{Cu-O2} \sim -0.18$  of the apical bond. This observation will be important later.

The presence of the anti-Jahn-Teller distorted doped  $CuO_6$  octahedra in the PTG calculations will manifest itself in an increased atomic displacement factor for O2, especially along  $z$ . The most sensitive parameter will be the width of the Cu-O pair distribution along the  $z$ -axis. This cannot be measured directly from the PDF because of peak overlap but can be found from the sum of  $U_{33}(Cu) + U_{33}(O2)$ . The mean-square width is plotted in Fig. 2 and does increase with increasing doping at constant temperature, a sign that static disorder associated with this bond is increasing with doping. To investigate more quantitatively whether this increase is consistent with the PTG predictions we calculated the PDF of a model structure containing the PTG defects. This simulated PDF was then fit using PDFFIT using the standard LTO model. This gives us a measure of how much  $U_{33}(O2)$  would increase in a standard LTO-structure refinement due to the presence of the PTG defects. The PDF was simulated for the  $x = 0.125$  composition using a 8x unit cell in the following way. The reference structure used was that of the undoped material with atomic positions taken from [3] and displacement factors taken from our PDF result for the undoped sample. One La in the supercell was then replaced with Sr and the atoms on the  $CuO_6$  octahedron adjacent to the Sr were displaced by

the  $\Delta$ -values from the PTG prediction given above. The displacement parameters in the model retained their values in the  $x = 0$  compound. This neglects strain due to the defects that would tend to increase displacement parameters further. The resulting PDFs were refined with the standard LTO unit cell. This resulted in an enlarged value of  $U_{33}(Cu) + U_{33}(O2) = 9.1 \times 10^{-3} \text{ \AA}^{-2}$  plotted on Fig. 2. This overestimates the observed displacement factors.

We now consider the expected structural changes that would occur based on electrostatic considerations in the conventional doping model. First, we note that the charge of the  $CuO_2$  plane is becoming less negative with doping which could result in the apical  $O^{2-}$  moving closer to the plane. A very rough estimate of this behavior is possible neglecting the Jahn-Teller effect and assuming an ionic picture by using ionic radii of  $O^{2-} = 1.35 \text{ \AA}$ ,  $Cu^{2+} = 0.73 \text{ \AA}$ ,  $Cu^{3+} = 0.54 \text{ \AA}$ ,  $La^{3+} = 1.16 \text{ \AA}$  and  $Sr^{2+} = 1.26 \text{ \AA}$  [10]. From this we get  $\Delta r_{Cu-O2} = -0.19 x$  and  $\Delta r_{La/Sr-O2} = 0.1 x$  which appear in Fig. 1 as dotted lines. Not surprisingly, these curves are similar to those predicted by PTG that is also a model involving a mixture of  $Cu^{2+}$  and  $Cu^{3+}$  sites. Uniform doping of charge into the Cu-O planes would not result in an increase in  $U_{33}(O2)$  on its own; however, the presence of misfitting  $Sr^{2+}$  dopant ions would. The fact that the observed increase in  $U_{33}(O2)$  exists but is smaller than needed to explain the PTG defects may argue in favor of this interpretation. There is a suggestion from single crystal refinements compared with empirical potential calculations that increases in displacement factors with doping can be explained in this way without invoking PTG-type defects [11]. Our results would tend to support this.

A more refined empirical framework for studying the distribution of charge between bonds is the bond valence model [12]. In this theory there is a direct relationship established between bond-length,  $r$ , and the amount of charge in a bond (the bond-valence,  $s$ ). Using this approach it is possible to determine how much of the doped charge is going into the planar vs. the apical bonds from a measurement of their length changes. The results are shown in Fig. 3. Here we plot how the total doped charge (assumed to be given by  $x$ ) distributes itself between the apical and planar orbitals respectively, as determined from the bond-valence sums. The dimensionless variables,  $\eta_p$  (solid circles) and  $\eta_a$  parameterize this partition where  $\eta_p + \eta_a = 1$ . Details of these calculations will be presented elsewhere [5]

As is apparent in Fig. 1, *both* the apical and in-plane bonds shorten with doping indicating a reduction in charge and doped holes going into both planar and apical bonds. However, one of the key aspects of this theory is the non-linear form of the bond valence,  $s(r)$ . As a result, the same amount of charge doped into a long-bond shortens it much more than it would a short-bond, and vice versa. At  $x = 0$   $r_{Cu-O1} < r_{Cu-O2}$  reflecting the

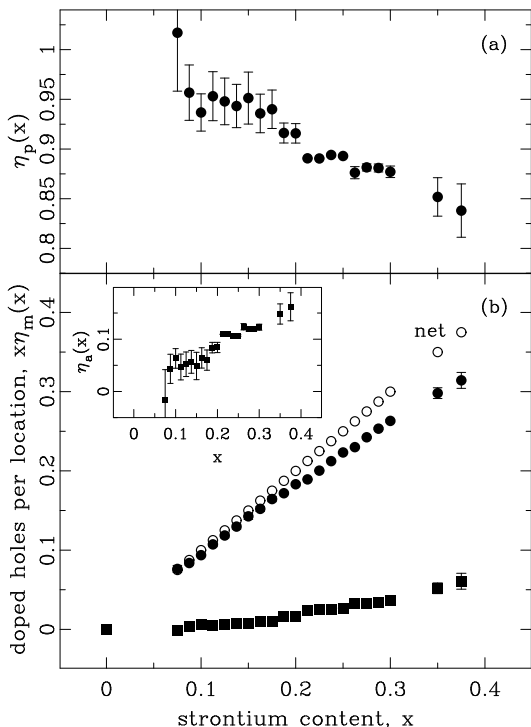


FIG. 3: (a) Partitioning parameter vs. Sr content. (b) Estimated average distribution of doped charge at 10 K based on bond valence calculations using Rietveld obtained distances: net apical share (solid squares), net planar share (solid circles), total doped charge (open circles). Inset: a measure of the amount of charge doped into the apical orbitals.

fact that initially the holes that make Cu in the 2+ state reside predominantly in the planar orbitals making these the canonical half-filled anti-bonding bands, with the apical bonds being doubly occupied with electrons (i.e., full, no holes). The physics of this is the existence of the Jahn-Teller distortion; however, this shows that the phenomenological bond-valence model is making the correct prediction for the charge segregation initially. Subsequently, the experimental observation is that *both the planar and apical bonds shorten at about the same rate* but because the planar bonds are initially shorter, and the fact that there are four of them rather than two, mean that the experimental observations demand that the doped charge is going predominantly into the planar orbitals as is evident in Fig. 3.

The main result of this analysis is that the simple picture of localized  $\text{Cu}_{3z^2-r^2}-\text{O}p_z$  doped holes associated with Sr sites described by the PTG calculations is not supported by the structural data. To a rather good approximation doped charge is going into the planar  $\text{Cu}_{x^2-y^2}-\text{O}p_{x,y}$  orbitals. This does not rule out localized doped defects if they have sufficient planar character. Such defects have been stabilized in the unrestricted Becke-3-Lee-Yang-Parr density functional calculations [13]. However, the observation that  $r_{\text{Cu}-\text{O}2}$  is

getting shorter also requires that some doped charge is appearing in the apical orbital and a correction should be made to the canonical  $p = x$  relationship to account for this, where  $p$  is the doped charge in the planar orbitals. The partitioning parameter  $\eta_p$  gives the correction. The number of doped holes in the planar bonds,  $p$ , is therefore given by  $p = x\eta_p$  ( $\eta_p$  shown in Fig. 3(a)). This augments spectroscopic measurements that show the partition of charge between copper and oxygen but struggle to differentiate partition between planar and apical bonds [14, 15]. Note that, at all dopings, greater than 85% of doped charge goes into the planar orbitals, though increasingly it appears in the apical bonds as doping increases.

In summary, we have tested the hypothesis that doping in  $\text{La}_{2-x}\text{Sr}_x\text{CuO}_4$  is occurring predominantly in  $\text{Cu}_{3z^2-r^2}-\text{O}p_z$  orbitals [1], rather than the canonical picture of doping into the planar  $\text{Cu}_{x^2-y^2}-\text{O}p_{x,y}$  bands. Whilst the average structure evolves *qualitatively* as would be predicted according to  $\text{Cu}_{3z^2-r^2}-\text{O}p_z$  doping picture, more quantitative analysis suggests that the canonical picture of one hole doped into the planar bands per strontium is actually rather close to the true situation. We present a correction factor quantifying the partition of doped charge between planar and apical bonds.

We would like to acknowledge M. J. Gutmann, A. Bianconi, N. L. Saini and P. G. Radaelli for help and discussions. We acknowledge beamtime on the instrument GEM at ISIS. This work was supported by NSF through grant DMR-0075149.

\* Electronic address: [billinge@pa.msu.edu](mailto:billinge@pa.msu.edu);  
URL: <http://www.totalscattering.org/>

- [1] J. K. Perry et al., Phys. Rev. B **65**, 144501 (2002).
- [2] D. Haskel et al., Phys. Rev. B **56**, R521 (1997).
- [3] P. G. Radaelli et al., Phys. Rev. B **49**, 4163 (1994).
- [4] E. S. Božin et al., Phys. Rev. B **59**, 4445 (1999).
- [5] E. S. Božin et al., unpublished.
- [6] A.C. Larson and R.B. Von Dreele, Los Alamos Nat. Lab. Rep. LAUR 86-748 (1994).
- [7] T. Egami and S. J. L. Billinge, *Underneath the Bragg Peaks: Structural analysis of complex materials*, Pergamon, Oxford, 2003.
- [8] P. F. Peterson et al., J. Appl. Crystallogr. **33**, 1192 (2000).
- [9] Th. Proffen and S. J. L. Billinge, J. Appl. Crystallogr. **32**, 572 (1999).
- [10] R. D. Shannon and C. T. Prewitt, Acta Cryst. B **25**, 925 (1969).
- [11] M. Braden et al., Phys. Rev. B **63**, 140510 (2001).
- [12] I. D. Brown and D. Altermatt, Acta Cryst. B **41**, 244 (1985).
- [13] J. Tahir-Kheli, private communication.
- [14] C. T. Chen et al., Phys. Rev. Lett. **66**, 104 (1991).
- [15] C. T. Chen et al., Phys. Rev. Lett. **68**, 2543 (1992).